

Papers published in *Hydrology and Earth System Sciences Discussions* are under open-access review for the journal *Hydrology and Earth System Sciences*

**Chloride deposition
mapping**

H. Guan et al.

Factors influencing chloride deposition in a coastal hilly area and application to chloride deposition mapping

H. Guan^{1,2}, A. J. Love^{1,3}, C. T. Simmons^{1,2}, and A. S. Kayaalp⁴

¹School of Chemistry, Physics and Earth Sciences, Flinders University, Adelaide, Australia

²National Centre for Groundwater Research and Training, Flinders University, Australia

³Department of Land, Water, and Biodiversity Conservation, South Australia

⁴Water Technology Division, Water Corporation, Western Australia

Received: 20 July 2009 – Accepted: 16 August 2009 – Published: 16 September 2009

Correspondence to: H. Guan (huade.guan@flinders.edu.au)

Published by Copernicus Publications on behalf of the European Geosciences Union.

Title Page

Abstract

Introduction

Conclusions

References

Tables

Figures

◀

▶

◀

▶

Back

Close

Full Screen / Esc

Printer-friendly Version

Interactive Discussion



Abstract

Chloride is commonly used as an environmental tracer for studying water flow and solute transport in the environment. It is especially useful for estimating groundwater recharge based on the commonly used chloride mass balance (CMB) method. Strong spatial variability in chloride deposition in coastal areas is one difficulty encountered in appropriately applying the CMB approach. Furthermore, intensive vegetation clearance for agriculture, for example during the European settlement in many coastal areas of Australia, may have perturbed catchment chloride balance conditions for appropriate use in CMB applications. In order to deal with these issues, a high resolution chloride deposition map in the coastal region is needed. In this study, we examined geographic, orographic, and atmospheric factors influencing chloride deposition in the Mount Lofty Ranges (MLR), a coastal hilly area of approximately 9000 km² spatial extent in South Australia, using partial correlation and regression analyses. The results indicate that coastal distance, and terrain aspect and slope are two most significant factors controlling chloride deposition. Coastal distance accounts for 65% spatial variability in chloride deposition, with terrain aspect and slope for 8%. The deposition gradient is about 0.08 gm⁻²year⁻¹ km⁻¹ as one progresses inland. The results are incorporated into a published de-trended residual kriging approach (ASOADeK) to produce a 1 km×1 km resolution annual chloride deposition map and a bulk precipitation chloride concentration map. The average uncertainty of the deposition map is about 30% in the western MLR, and over 50% in the eastern MLR. The maps will form a very useful basis for examining catchment chloride balances for use in the CMB application in the study area.

1 Introduction

Chloride is commonly used as an environmental tracer for studying water flow and solute transport in surface water bodies, vadose zones and aquifers, and is especially

HESSD

6, 5851–5880, 2009

Chloride deposition mapping

H. Guan et al.

Title Page

Abstract

Introduction

Conclusions

References

Tables

Figures

◀

▶

◀

▶

Back

Close

Full Screen / Esc

Printer-friendly Version

Interactive Discussion



useful to estimate groundwater recharge based on chloride mass balance (CMB) (Eriksson and Khunakasem, 1969; Walker et al., 1991; Cook et al., 1992; Phillips, 1994; Kirchner et al., 2000; Edmunds et al., 2002; Scanlon et al., 2002). A typical CMB formula is shown as

$$C_p P = C_g G + C_r R \quad (1)$$

where C_p is chloride concentration in bulk precipitation, P is precipitation in the catchment, C_g is chloride concentration in groundwater G that was recharged from the catchment, C_r is chloride concentration in the stream runoff R carrying water out of the catchment. One primary assumption of the CMB method is that chloride in the catchment is in equilibrium with current atmospheric forcing. Otherwise chloride would accumulate in the soil or be leached out of soil from the historical storage, breaking down the chloride mass balance between current precipitation and recharged groundwater. Because the CMB method does not require knowledge of dynamic hydrological processes, it provides a good solution to estimate groundwater recharge in mountainous terrain where hydrogeological and hydrometeorological conditions are complex (Wilson and Guan, 2004). In order to reasonably estimate groundwater recharge using the CMB method, the atmospheric chloride input in bulk precipitation must be known. In the inland area, atmospheric chloride deposition does not change much over a large distance (e.g., ~100 km) (Keywood et al., 1997). One estimate of average chloride deposition either directly from bulk precipitation sampling, or inferred from the ratio of $^{36}\text{Cl}/\text{Cl}$ (Scanlon, 2000) which has a 30% uncertainty, is often used in the CMB calculation. In the coastal area, however, large spatial variability of chloride deposition is often observed (Keywood et al., 1997; Kayaalp, 2001; Biggs, 2006). A detailed map of atmospheric chloride deposition is thus needed to apply the CMB approach for estimating groundwater recharge in the coastal areas where large spatial variability in chloride deposition occurs (Alcala and Custodio, 2008).

It is commonly accepted that the primary source of the atmospheric chloride is from the ocean by wind-induced whitecaps and bursts, which inject sea water drops into the atmosphere (Lewis and Schwartz, 2004). About 10% of total chloride in the sea

Chloride deposition mapping

H. Guan et al.

Title Page

Abstract

Introduction

Conclusions

References

Tables

Figures

◀

▶

◀

▶

Back

Close

Full Screen / Esc

Printer-friendly Version

Interactive Discussion



Chloride deposition mapping

H. Guan et al.

Title Page

Abstract

Introduction

Conclusions

References

Tables

Figures

◀

▶

◀

▶

Back

Close

Full Screen / Esc

Printer-friendly Version

Interactive Discussion



salt aerosols moves into the continents, and the majority of this chloride is deposited within 100 km of the coastal area (Eriksson, 1959, 1960). Two primary mechanisms, dry deposition and wet deposition, control chloride removal from the atmosphere to the land surface. Chloride-bearing aerosols can settle down to the surface by gravitational forces. This dry deposition process is highly dependent on wind conditions and the aerosol size. Chloride in the aerosols can also be rained out from the cloud, or washed out by the falling rain drops. This wet deposition process is dependent on precipitation characteristics. In terms of hydrological applications, it is the total chloride deposition (chloride deposition hereafter), i.e., the sum of wet and dry depositions, that is important because it gives the input chloride for the CMB calculation (Wood and Sanford, 1995). Thus, chloride deposition is usually measured from accumulated rain samples over a certain period, with samplers sitting in an open area, and open to the sky all the time. As chloride-bearing aerosols originate from the ocean, it is typically observed that chloride deposition over the continents decays exponentially with increasing distance from the coast (coastal distance hereafter) (Keywood et al., 1997; Gustafsson and Larsson, 2000).

This coastal distance dependence, when quantitatively determined, is useful to estimate chloride deposition for a point location at some known distance from the coast. However, deposition processes are also associated with the prevailing wind direction and it is therefore difficult to use the distance-dependence function alone to construct good resolution chloride deposition maps. Instead, kriging is frequently used to map chloride deposition. Gustafsson and Larsson (2000) applied ordinary block kriging to construct 10 km×10 km resolution seasonal chloride deposition maps with 49 data points over an area of $8 \times 10^4 \text{ km}^2$ in Southern Sweden. Alcala and Custodio (2008) used ordinary kriging to produce 10 km×10 km mean annual chloride deposition map with measurements at over 200 geographic points for continental Spain ($5 \times 10^5 \text{ km}^2$). A reliable kriging requires an appropriate sampling density and distribution (Chang et al., 1998), which is, however, often lacking in reality. Can we incorporate some associated physical process information, including coastal distance dependence, so as

to make more reliable estimates for chloride deposition to form a basis for chloride deposition mapping? Similar approaches have been successfully applied in precipitation and rain water isotope mapping in mountainous terrain (Guan et al., 2005, 2009). In this study, we aim to examine the influencing factors associated with physical processes that control chloride deposition. This understanding will aid in producing more robust chloride deposition maps in coastal areas, where chloride deposition can often vary significantly even over a few kilometres (Kayaalp, 2001). The results will be used to construct a chloride deposition map and a bulk precipitation chloride concentration map at a spatial resolution of 1 km×1 km over an area of 9000 km², using a de-trended residual kriging approach. Similar approach has been used in precipitation mapping (Guan et al., 2005, 2009).

The study is based on the Mount Lofty Ranges (MLR) of South Australia, which provides about 60% of the water supply to the Adelaide Metropolitan area. Our starting hypotheses are that in addition to coastal distance, (1) windward slopes, associated with sea breeze and in-coming moisture direction, enhance chloride deposition due to topographic interception, and (2) elevation/altitude enhances chloride deposition due to increasing precipitation. We will show that terrain slope and aspect, associated with prevailing wind direction, do indeed influence chloride deposition in the coastal area, but in a manner that is contrary to our starting hypothesis. This result is helpful to improve our understanding of sea salt deposition in the coastal area. They may also be useful for studying pollutant deposition in mountainous areas in close proximity to pollution sources. These new findings are incorporated into chloride deposition mapping for the study area, where intensive native vegetation clearance for agriculture occurred some 100 to 150 years ago. The abrupt land cover change has changed the land surface boundary condition, posing a question whether the current system has reached new chloride equilibrium condition for the CMB application. The chloride map produced here will be used to examine the catchment chloride balance states, which is to be discussed in a subsequent paper.

Chloride deposition mapping

H. Guan et al.

Title Page

Abstract

Introduction

Conclusions

References

Tables

Figures

◀

▶

◀

▶

Back

Close

Full Screen / Esc

Printer-friendly Version

Interactive Discussion



2 Methodology

2.1 Study area and data

The study area lies to the east of Adelaide, South Australia (Fig. 1). It covers an area of about 9000 km², with topographic relief of 700 m. To the west is Gulf St Vincent, which is about 150 km long and 70 km wide. To the south is the Southern Ocean, with saline lake Alexandria sitting to the southwest. The climate is of Mediterranean type, with wet winters and dry summers. The annual precipitation ranges from below 300 mm to above 1000 mm, with an areal average of 600 mm. Prevailing westerly moisture flux feeds precipitation (Guan et al., 2009), and thus wet chloride deposition in the area.

Westerly sea breezes occur frequently during part of the day (Fig. 2) over most of the study area, which fuel atmospheric transport of sea salt aerosols from the Gulf St Vincent and facilitate dry chloride deposition. At the south edge of the area, no dominant southerly wind is observed. Thus, from both wet and dry deposition points of view, atmospheric chloride aerosols come from the west. Chloride concentration in bulk precipitation was measured at 17 sites, over two periods by two organizations: Flinders University (1992–1994) and Department of Water, Land and Biodiversity Conservation (DWLBC) (2002–2005) (Table 1). DWLBC samples were multiple-month cumulative rain, while Flinders samples were monthly cumulative rain. A thin layer of mineral oil was applied in the collectors to avoid water evaporation. On average the sampling period is about 2 years, with two sites (Sites 4 and 5) sampled for shorter than one year. They are nevertheless included because the sampling period covers both halves of the dry and rainy seasons. Both rain sample volume and chloride concentration were measured for each cumulative sample. Chloride concentration was measured at Land and Water Division of the Commonwealth Scientific and Industrial Research Organization, Adelaide, Australia. Average chloride concentrations and annual chloride deposition are calculated from samples at each of the 17 sites (Table 1). In addition, wind speed and wind direction data for 41 sites in and near the study area were obtained from the Bureau of Meteorology of Australia (BOM) (Fig. 1). Wind speed was recorded as a

Chloride deposition mapping

H. Guan et al.

Title Page

Abstract

Introduction

Conclusions

References

Tables

Figures

◀

▶

◀

▶

Back

Close

Full Screen / Esc

Printer-friendly Version

Interactive Discussion



daily mean for the horizontal component, and wind direction was recorded twice daily at 09:00 a.m. and 03:00 p.m. local time.

2.2 Correlation analysis

Correlation analysis has been widely used to examine linear association between variables. The Pearson product-moment correlation coefficient (r) is the most common measure of linear association between two variables. An r value close to +1 or -1 often (but not always) indicates some physical causal relationship between the two variables, while an r value close to zero indicates no physically causal relation. When multiple variables are correlated to one another, the correlation coefficient of the variable of interest with any one of the other variables may give association implication which is not physically dependent. To solve this problem, a partial correlation coefficient is applied to examine the linear correlation between the two variables with the effects of other selected variables removed (Lowry, 1999–2009). An example of partial correlation coefficient between variables x and y independent of a third variable (z) is calculated using

$$r_{xy(z)} = \frac{r_{xy} - r_{xz}r_{yz}}{\sqrt{1 - r_{xz}^2}\sqrt{1 - r_{yz}^2}} \quad (2)$$

where r is Pearson correlation coefficient between the two variables denoted in the subscripts. The MATLAB function *partialcorr* is used to calculate partial correlation coefficients in this study. After r is obtained, the significance is tested with a t -distribution. The t -value is calculated by

$$t = \frac{r}{\sqrt{(1 - r^2)/(N - 2)}} \quad (3)$$

where N (≥ 6) is the number of samples. This significance test is applied to examine our two hypotheses, one relating to the elevation effect and the other relating to terrain

Chloride deposition mapping

H. Guan et al.

Title Page

Abstract

Introduction

Conclusions

References

Tables

Figures

◀

▶

◀

▶

Back

Close

Full Screen / Esc

Printer-friendly Version

Interactive Discussion



aspect effect on chloride deposition. If the tested factor is important in chloride deposition, the partial correlation coefficient between chloride deposition and the factor variable should be statistically significant.

2.3 ASOAdEK regression and mapping

5 A multivariate regression embedded in a geostatistical model (Auto-searched Orographic and Atmospheric effects De-trended Kriging, or ASOAdEK) has been shown to successfully capture orographic effects on precipitation distribution over mountain terrains (Guan et al., 2005). The ASOAdEK regression was originally developed to auto-search the effects of atmospheric moisture gradient, prevailing moisture flux direction
10 associated terrain aspect and slope, and terrain elevation, on precipitation distribution. Recently, it was applied to examine orographic effects on rain isotope distribution (Guan et al., 2009). Since wet chloride deposition occurs with precipitation, and dry chloride deposition over the area has similar westerly source as precipitation, we attempt to use the ASOAdEK regression to examine the effects of selected topographic variables
15 on chloride deposition. The original regression model, including both elevation and terrain aspect, can be found in (Guan et al., 2005). The regression model used below including elevation, terrain aspect and slope, first appears in (Guan et al., 2009).

$$D = b_0 + b_1X + b_2Y + b_3Z + b_4\beta \cos \alpha + b_5\beta \sin \alpha \quad (4)$$

where D is annual chloride deposition (gm^{-2}), X and Y are geographic coordinates
20 (usually as easting and northing in the Universal Transverse Mercator (UTM) coordinate system, in km), used to capture the effect of coastal distance dependence, Z is above-sea-level terrain elevation in kilometres, β is the slope angle in degree, α is the terrain aspect, defined as the direction of slope orientation, zero to the north, increasing clockwise, and 180 to the south. The two trigonometric terms are derived from
25 $\cos(\alpha - \omega)$, where ω is the source flux direction. This function has a value of 1 at windward slopes, and -1 at leeward slopes. This formulation was originally designed to

Chloride deposition mapping

H. Guan et al.

Title Page

Abstract

Introduction

Conclusions

References

Tables

Figures

◀

▶

◀

▶

Back

Close

Full Screen / Esc

Printer-friendly Version

Interactive Discussion



capture the orographic effect of more precipitation (or chloride deposition) on the windward slope than on the leeward side. If chloride deposition is enhanced in the leeward side, the sign of b_4 and b_5 will be reversed.

After regression is performed, it is used to generate a regression estimate map (the trend) based on a DEM. The difference between the observations and regression estimates are then used to generate a de-trended residual map. The final chloride deposition map is the sum of the regression map and the residual map. This procedure is simply called ASOAdEK mapping. More details on this approach can be found in (Guan et al., 2005). The performance of this mapping approach is examined by cross validation, in which each of the total N data points is set aside each time to compare with the mapping estimate at the location based on the remaining $(N-1)$ data points (Isaaks and Srivastava, 1989). It is also compared to direct ordinary kriging of the observed chloride depositions. It is called direct kriging, to be distinguished from the residual kriging, which is one component of ASOAdEK mapping approach. All kriging calculations are performed with Geostatistical Software Library (Deutsch and Journel, 1998). Finally, the bulk precipitation chloride concentration map is then constructed based on the annual chloride deposition map and annual precipitation map of the study area, both at a spatial resolution of $1 \text{ km} \times 1 \text{ km}$.

3 Results

3.1 Correlation analysis and hypothesis testing

As discussed in Sect. 2.1, both wet and dry chloride deposition in the study area comes from a westerly direction. Chloride deposition data of most of the 17 sites (Table 1, Fig. 3) follows this trend. However, at sites 16 and 17, chloride deposition is abnormally high in comparison to site 15. This could be due to an additional local chloride source, or short-range transport of chloride aerosol from Lake Alexandrina and the Southern Ocean that only locally influences the southeastern corner of the area. Thus,

Chloride deposition mapping

H. Guan et al.

Title Page

Abstract

Introduction

Conclusions

References

Tables

Figures

◀

▶

◀

▶

Back

Close

Full Screen / Esc

Printer-friendly Version

Interactive Discussion



Chloride deposition mapping

H. Guan et al.

Title Page

Abstract

Introduction

Conclusions

References

Tables

Figures

◀

▶

◀

▶

Back

Close

Full Screen / Esc

Printer-friendly Version

Interactive Discussion



5 sites 16 and 17 are excluded from correlation and regression analysis, to avoid their anomalous disturbance on investigating the physical processes common to the whole area. However, sites 16 and 17 are included for residual kriging and to generate the chloride deposition map. Although an exponential decrease in chloride deposition (D) with increasing coastal distance (approximately X in the study area) is reported at a large scale (Keywood et al., 1997; Gustafsson and Larsson, 2000), a linear relationship is observed between D and X in the study area with coastal distance within 100 km (Fig. 3). This feature supports the fact that a linear correlation and regression analyses between D and X is appropriate over the study area.

10 With sites 16 and 17 excluded, the correlation matrix of chloride deposition with precipitation and five selected variables (used as predictor variables in ASOADEK regression) (Table 2) suggests that Z and $\beta \cos \alpha$ are not significantly correlated to D . Based on a one-tailed t test, $|r|$ needs to be 0.44 for a significant level at $p=0.05$, and 0.35 for $p=0.10$. D and X (easting) have the highest negative correlation. This is consistent with the westerly chloride source for the study area and coastal distance-dependent chloride deposition reported in the literature. D is moderately positively correlated with P (precipitation). Because Y (northing) and $\beta \sin \alpha$ are both highly correlated with X , it is difficult to evaluate their association with D based on the correlation matrix. Partial correlation coefficients (Fig. 4), with the effect of X removed, suggest that Y and P are not significantly associated with D , while $\beta \sin \alpha$ is, with significant level at $p=0.04$ (one-tailed t test) (Fig. 4), implying slope and aspect dependent chloride deposition. With X and P effect removed, the correlation between D and $\beta \sin \alpha$ is significant at $p=0.06$, suggesting that dry deposition is also significant associated with terrain aspect. With precipitation effect removed, partial correlation coefficient between D and X is -0.76 , suggesting that dry deposition has a similar coastal-distance dependence as wet deposition. Partial correlation analysis results confirm the insignificant association between D and Z , and between D and $\beta \cos \alpha$.

25 We now examine the two hypotheses, (1) elevation and (2) west-facing slope facilitating chloride deposition, as they pertain to possible topographic influences on chlo-

ride deposition. Elevation apparently does not enhance chloride deposition, as no significant linear association is found from either the correlation matrix or the partial correlation analysis. Terrain aspect and slope are significant factor, as indicated by the correlation between D and $\beta \sin \alpha$. The partial correlation coefficient between the two variables is positive. Based on the definition of terrain aspect α in Eq. (4), it has a positive value on east-facing slopes. This indicates that more chloride deposition occurs on leeward slopes in respect to the atmospheric chloride source direction, instead of on the windward slopes in our starting hypothesis.

3.2 Regression analysis and ASOAdEK mapping

Based on partial correlation analysis, among the five predictor variables in Eq. (4), D is significantly linearly associated with X and $\beta \sin \alpha$. Thus, regression is performed with X and $\beta \sin \alpha$ only (Table 3). The results indicate that coastal distance explains about 65% of the spatial variability in chloride deposition in the study area, while terrain aspect accounts for an additional 8%. Based on the regression results, the chloride deposition gradient is about $0.08 \text{ gm}^{-2} \text{ year}^{-1} \text{ km}^{-1}$ downwind away from the coast. This value is slightly smaller than the values of $0.2\text{--}2 \text{ gm}^{-2} \text{ year}^{-1} \text{ km}^{-1}$ reported for Spain's coastal areas (Alcala and Custodio, 2008). This possibly pertains to wind climate in the study area, to be discussed later.

After regression is performed, it can be used to construct a chloride deposition regression map and ASOAdEK map. To examine the mapping performance, cross validation was performed in comparison to the direct ordinary kriging (Fig. 5a). In comparison to direct kriging, both regression and ASOAdEK estimates give a smaller mean absolute error (MAE), and higher correlation coefficient between the estimates and observations. Cross-validation semivariogram for direction kriging is included in Fig. 6a, because it is similar among 17 sets of cross-validation data points, and is not shown for residual kriging because the semivariogram is different among 15 sets of cross-validation data points. The MAE value of regression is 0.80 g/m^2 , about 20% of average observation values over the first 15 locations in Table 1, and the MAE value

Title Page

Abstract

Introduction

Conclusions

References

Tables

Figures

◀

▶

◀

▶

Back

Close

Full Screen / Esc

Printer-friendly Version

Interactive Discussion



of ASOAdEK cross validation is 0.84 g/m^2 , about 21% of the observation average. ASOAdEK cross validation results slightly degrades in comparison to that of the regression, probably because the chloride network density is too low. The residual kriging is nevertheless applied because sites 16 and 17 were not included in the regression. Comparison of cross validations provides us confidence to construct chloride deposition map using ASOAdEK method. The various maps derived from ASOAdEK mapping approach are included in Fig. 7a–d. The regression map (Fig. 7a) underestimates chloride deposition in the southeastern corner of the area, because the two data points (16 and 17 in Table 1) were not included in the regression. The underestimates are compensated by large positive residuals in Fig. 7b. The chloride deposition map (Fig. 7c) is constructed as the sum of regression and residual maps. The sum of square-root of kriging variance, and regression uncertainty interval at $p=0.05$, is provided as an indicator for mapping uncertainty (Fig. 7d), mainly showing the sampling site distribution effect. Overall, annual chloride deposition rate is over 6 gm^{-2} in the southwestern corner and western coast, decreasing to $4\text{--}5 \text{ gm}^{-2}$ in the central part, and to below 2 gm^{-2} in the eastern and northeastern edges of the area. The average uncertainty in the western half is some 1 gm^{-2} , about 20% of the estimated chloride deposition, while in the eastern half, average uncertainty is over 2 gm^{-2} , about 50% of the estimated chloride deposition. This value is similar or larger than the cross-validation MAE values, suggesting that uncertainty intervals shown in Fig. 7d are conservative. The uncertainty at and near the sampling sites is small. The mean absolute error of the regression estimates over the 15 sites is 0.54 gm^{-2} , equivalent to 14% of the average observed annual chloride deposition at these sites (Table 3) (Fig. 5b). After the residual kriging is added, the mean absolute error over the 17 sites is reduced to 0.41 gm^{-2} , about 11% of the average observed annual deposition (Fig. 5b). Finally, a bulk precipitation chloride concentration map (Fig. 7e) and its uncertainty (Fig. 7f) are provided. In comparison to chloride sampling, the precipitation observation network is much denser (94 gauges) and covers a much longer period (the majority of these data have over 30 years record) (Guan et al., 2009). The uncertainty in the precipita-

**Chloride deposition
mapping**

H. Guan et al.

Title Page

Abstract

Introduction

Conclusions

References

Tables

Figures

◀

▶

◀

▶

Back

Close

Full Screen / Esc

Printer-friendly Version

Interactive Discussion



tion mapping is neglected when chloride concentration uncertainty is calculated. The map (Fig. 7e) shows that chloride concentration in bulk precipitation is about 5 mg/l, increases westward toward the coast and southeast-ward, to above 10 mg/l. The uncertainty in bulk precipitation chloride concentration is 1–2 mg/l for the central of the MLR, about 30% of estimated chloride concentration (Fig. 7f). This level of uncertainty is similar to that using much expensive $^{36}\text{Cl}/\text{Cl}$ method (Scanlon, 2000). However, due to the sparse sample points in the eastern part of the study area, the uncertainty is around and above 50% of the estimated chloride concentration. More sampling points are recommended for the future in this portion of the area.

4 Discussion

It is interesting to observe that elevation does not significantly influence chloride deposition, although it enhances precipitation in the study area (Guan et al., 2009). Correlation coefficient between P and Z is 0.79, but it is only -0.03 between D and Z (Table 2). This suggests either that chloride wet deposition does not increase proportionally with precipitation, or that the increase in wet deposition with elevation is compensated by a decrease in dry deposition with elevation, or both. Chloride concentration in instantaneous rain samples may give us some hint on how wet deposition is related to precipitation rate. A series of 1.6-mm rain samples were collected over a period with a single rainfall event (about 30 mm precipitation) on Flinders University campus on 5 May 2008 (Fig. 8). It is observed that chloride concentration varies in a range between 3 and 17 mg/l. During the seven hour period, chloride concentration peaks at 09:00, 11:30, and 15:40. The subsequent rain samples after the peak time have lower chloride concentration. This indicates that the peak concentration samples were probably condensed earlier in the source cloud which dissolved more chloride-bearing aerosols, with the subsequent rain drops having less chloride aerosols to include. If we assume a similar mechanism applies to the whole area, it is easy to understand why wet chloride deposition does not increase proportionally with precipitation. This is supported by

Chloride deposition mapping

H. Guan et al.

Title Page

Abstract

Introduction

Conclusions

References

Tables

Figures

◀

▶

◀

▶

Back

Close

Full Screen / Esc

Printer-friendly Version

Interactive Discussion



the weak partial correlation between chloride deposition (D) and precipitation (P) when coastal distance (X) effect is removed (Fig. 4). Nevertheless, D is positively correlated (although not statistically significant, $r=0.21$) to elevation (Z) when X effect is removed, suggesting elevation does weakly facilitate wet deposition, by increasing precipitation, but not in the same proportion to its effect on increasing precipitation. When X and P effect is removed, partial correlation between D and Z becomes negative. This result indicates that dry deposition slightly decreases with elevation. As elevation affects both wet and dry deposition in an opposite way, the chloride deposition becomes elevation-independent in the study area.

Another interesting finding is that chloride deposition in the east-facing slope is significantly larger than the west-facing slope when coastal distance effect is removed. Previously, we thought that the western slope, facing incoming chloride-bearing aerosols flux, might intercept atmospheric chloride and enhance deposition. This hypothesis is not supported by the correlation analysis results. After careful analysis of wind direction in the study area, we find that due to land-sea wind circulation, westerly and easterly winds frequently occur within a day over the study area, but vary spatially and seasonally (Fig. 9). This may explain why the eastern slope facilitates chloride deposition. In Fig. 9, average sine values of wind direction at 09:00 a.m. and 03:00 p.m. are plotted against the longitude, for summer and winter seasons. The sine value is positive if the wind comes from the east, and negative if the wind comes from the west. The wind directions at 09:00 a.m. and 03:00 p.m. are approximately representative for the wind in the night time and daytime, respectively. In summer, westerly winds dominate during the daytime, especially to the west of longitude 138.7° E. In the night time, easterly winds occur to the west of 139.0° E. In winter, westerly winds are persistent in the day time throughout the area, with weak easterly winds only occurring to the west of 138.6° E. For both seasons, during the day time, westerly winds carry chloride-bearing aerosols from the St. Vincent Gulf inland. This may explain a slightly lower chloride deposition gradient in the study area, in comparison to other areas. When the westerly air mass is constrained by the topographic barrier on the western slope,

Chloride deposition mapping

H. Guan et al.

Title Page

Abstract

Introduction

Conclusions

References

Tables

Figures

◀

▶

◀

▶

Back

Close

Full Screen / Esc

Printer-friendly Version

Interactive Discussion



Chloride deposition mapping

H. Guan et al.

Title Page

Abstract

Introduction

Conclusions

References

Tables

Figures

◀

▶

◀

▶

Back

Close

Full Screen / Esc

Printer-friendly Version

Interactive Discussion



windspeed increases, and reaches the maximum at the upwind side of the hill. The windspeed decreases over the down wind slope. This phenomenon has been extensively studied in sand dune formation processes (Andreotti et al., 2002). The elevated wind speed at the upwind slope facilitates atmospheric chloride transport, and a decreased wind speed at the downwind slope facilitates chloride deposition, explaining the positive partial correlation between D and $\beta \sin \alpha$ from the data. Similar mechanisms would apply to not only chloride depositions but also to other aerosol (pollutant) deposition in the mountain terrains which are in close proximity to industrial/urban air pollutant sources. During the night time, situations are different seasonally. In winter, easterly winds only happen to the west of the MLR, which may re-activate some previously deposited chloride to the atmosphere and return some atmospheric chloride back to the ocean, resulting in smaller dry deposition in the western slope, enhancing the difference in chloride deposition between the east-facing and west-facing slopes. In summer, easterly wind occurs over both western and eastern MLR, its effects on chloride deposition should be similar at both sides.

5 Conclusions

Chloride deposition in the Mount Lofty Ranges, a coastal hilly area in South Australia, was examined with selected geographical (easting and northing), orographic (elevation, slope and aspect), and atmospheric (precipitation) variables. Both partial correlation analysis and regression analysis were performed to understand the controlling factors in annual chloride deposition. The results indicate that the easting value of the site (equivalent to coastal distance), and terrain aspect and slope are two significant factors controlling chloride deposition. Coastal distance accounts for about 65% of the spatial variability in chloride deposition, with terrain aspect and slope accounting for about 8%. The deposition gradient is about $0.08 \text{ gm}^{-2} \text{ year}^{-1} \text{ km}^{-1}$ inland, slightly lower than the values reported for other areas, probably related to persistent day-time sea breeze. The correlation results suggest that chloride deposition is facilitated on

**Chloride deposition
mapping**

H. Guan et al.

the leeward slope in respect to the chloride aerosol source direction, which is likely related to larger wind speed on the upwind slope than on the downwind slope. The results also indicate that elevation slightly enhances wet deposition via increasing precipitation, but not in proportion to its effect on precipitation. Meanwhile, dry deposition is slightly weaker at higher elevations. These two opposite effects result in apparent elevation-independent chloride deposition in the study area.

Based on the regression analysis results, a published de-trended residual kriging mapping procedure (ASOAdEK) was applied to construct the annual chloride deposition map and bulk precipitation chloride concentration map. The average uncertainty of the deposition map is about 30% in the western MLR, comparable to that of the $^{36}\text{Cl}/\text{Cl}$ method, and over 50% in the eastern MLR where more future sampling is recommended. The maps will be useful to examine catchment chloride balance for the CMB application in the study area, which will be the subject of a separate paper.

Acknowledgements. Constructive discussion with Graham Green is appreciated. The Department of Water, Land and Biodiversity Conservation of South Australia provided some precipitation chloride data, and GIS layers. Bureau of Meteorology provided long-term precipitation data, and wind speed data. Stacey Priestley (Flinders University), Darren Ray (BOM), Tania Wilson, Graham Green, and Eddie Banks (DWLBC) and Russell Jones (Water Data Services), assisted in data preparation.

References

- Alcala, F. J. and Custodio, E.: Atmospheric chloride deposition in continental Spain, *Hydrol. Process.*, 22(18), 3636–3650, 2008.
- Andreotti, B., Claudin, P., and Douady, S.: Selection of dune shapes and velocities – Part 1: Dynamics of sand, wind and barchans, *Eur. Phys. J. B*, 28(3): 321–339., 2002.
- Biggs, A. J. W.: Rainfall salt accessions in the Queensland Murray-Darling Basin, *Aust. J. Soil Res.*, 44(6), 637–645, 2006.
- Chang, Y. H., Scrimshaw, M. D., Emmerson, R. H. C. and Lester, J. N.: Geostatistical analysis of sampling uncertainty at the Tollesbury Managed Retreat site in Blackwater Estuary, Essex,

[Title Page](#)[Abstract](#)[Introduction](#)[Conclusions](#)[References](#)[Tables](#)[Figures](#)[I◀](#)[▶I](#)[◀](#)[▶](#)[Back](#)[Close](#)[Full Screen / Esc](#)[Printer-friendly Version](#)[Interactive Discussion](#)

UK: Kriging and cokriging approach to minimise sampling density, *Sci. Total Environ.*, 221(1): 43–57, 1998.

Cook, P. G., Edmunds, W. M. and Gaye, C. B.: Estimating paleorecharge and paleoclimate from unsaturated zone profiles, *Water Resour. Res.*, 28(10), 2721–2731, 1992.

5 Deutsch, C. V. and Journel, A. G.: *GSLIB – Geostatistical Software Library and User's Guide*, Applied Geostatistics Series, Oxford University Press, New York, 369 pp., 1998.

Edmunds, W. M., Fellman, E., Goni, I. B., and Prudhomme, C.: Spatial and temporal distribution of groundwater recharge in northern Nigeria, *Hydrogeol. J.*, 10(1), 205–215., 2002.

10 Eriksson, E.: The yearly circulation of chloride and sulphur in nature; meteorological, geochemical and pedological implications, *Tellus*, 11(4), 375–403, 1959.

Eriksson, E.: The yearly circulation of chloride and sulphur in nature; meteorological, geochemical and pedological implications, Part 2, *Tellus*, 12, 63–109., 1960.

Eriksson, E. and Khunakasem, V.: Chloride concentrations in groundwater, recharge rate and rate of deposition of chloride in the Israel coastal plain, *J. Hydrol.*, 7, 178–197, 1969.

15 Guan, H., Simmons, C. T., and Love, A. J.: Orographic controls on rain water isotope distribution in the Mount Lofty Ranges, South Australia, *J. Hydrol.*, 372, 255–264, doi:10.1016/j.jhydrol.2009.06.018, 2009.

20 Guan, H., Wilson, J.L. and Makhnin, O.: Geostatistical mapping of mountain precipitation incorporating autosearched effects of terrain and climatic characteristics, *J. Hydrometeorol.*, 6(6), 1018–1031, 2005..

Gustafsson, M. E. R. and Larsson, E. H.: Spatial and temporal patterns of chloride deposition in Southern Sweden, *Water Air Soil. Poll.*, 124(3–4), 345–369, 2000.

Isaaks, E. H. and Srivastava, R. M.: *Applied Geostatistics*, Oxford University Press, UK, Inc, 561 pp., 1989.

25 Kayaalp, A. S. Application of rainfall chemistry and isotope data to hydro-meteorological modelling, Ph.D. Thesis, Flinders University, Adelaide, Australia, 273 pp., 2001.

Keyword, M. D., Chivas, A. R., Fifield, L. K., Cresswell, R. G. and Ayers, G. P.: The accession of chloride to the western half of the Australian continent, *Aust. J. Soil. Res.*, 35(5), 1177–1189, 1997.

30 Kirchner, J. W., Feng, X. H. and Neal, C.: Fractal stream chemistry and its implications for contaminant transport in catchments, *Nature*, 403(6769), 524–527, 2000.

Lewis, E. R. and Schwartz, S. E.: *Sea Salt Aerosol Production: Mechanisms, Methods, Measurements and Models – A Critical Review*, Geoph. Monog. Series, 152, American Geophys-

HESSD

6, 5851–5880, 2009

Chloride deposition mapping

H. Guan et al.

Title Page

Abstract

Introduction

Conclusions

References

Tables

Figures

◀

▶

◀

▶

Back

Close

Full Screen / Esc

Printer-friendly Version

Interactive Discussion



ical Union, Washington, DC, 413 pp., 2004.

Lowry, R.: Concepts and Applications of Inferential Statistics. <http://faculty.vassar.edu/lowry/webtext.html>, Vassar College, Poughkeepsie, NY, USA, 1999–2009.

Phillips, F. M.: Environmental tracers for water movement in desert soils of the American southwest, *Soil Sci. Soc. Am. J.*, 58(1), 15–24, 1994.

Scanlon, B. R.: Uncertainties in estimating water fluxes and residence times using environmental tracers in an arid unsaturated zone, *Water Resour Res.*, 36(2), 395–409, 2000.

Scanlon, B. R., Healy, R. W. and Cook, P. G.: Choosing appropriate techniques for quantifying groundwater recharge, *Hydrogeol. J.*, 10(1), 18–39, 2002.

Walker, G. R., Jolley, I. D., and Cook, P.G.: A new chloride leaching approach to the estimation of diffuse recharge following a change in land use, *J. Hydrol.*, 128, 49–67, 1991.

Wilson, J. L. and Guan, H.: Mountain-block hydrology and mountain-front recharge, in: *Groundwater Recharge in a Desert Environment: The Southwestern United States*, edited by: Hogan, J. F., Phillips, F. M., and Scanlon, B.R., Water Science and Applications Series, American Geophysical Union, Washington, DC, 113–137, 2004.

Wood, W. W. and Sanford, W. E.: Chemical and isotopic methods for quantifying groundwater recharge in a regional, semiarid environment, *Ground Water*, 33(3), 458–468., 1995.

HESSD

6, 5851–5880, 2009

Chloride deposition mapping

H. Guan et al.

Title Page

Abstract

Introduction

Conclusions

References

Tables

Figures

◀

▶

◀

▶

Back

Close

Full Screen / Esc

Printer-friendly Version

Interactive Discussion



Chloride deposition mapping

H. Guan et al.

Table 1. Chloride deposition and concentration over the Mount Lofty Ranges calculated from samples collected over two periods by DWLBC (1–8) and Flinders University (9–17).

ID	Site id	Site name	Easting (m)	Northing (m)	Data period m/y-m/y	Weight mean (mg/l)	Simple mean (mg/l)	Deposition (g/m ² /yr)
1	AW503502	Scott Creek	287895	6113235	02/03–02/05	5.4	5.0	4.05
2	AW426638	Mount Barker	306288	6117246	11/02–11/04	6.1	5.8	4.63
3	AW504512	Mt Pleasant	319631	6148870	12/02–10/03	5.2	5.2	2.57
4	AW504559	Cherryville	295316	6134505	01/03–07/03	4.2	4.2	4.37
5	AW504563	Milbrook	300896	6143374	07/03–03/04	5.9	5.8	3.65
6	AW505517	Penrice	321661	6184765	12/03–11/04	4.1	3.7	1.98
7	AW505537	Mount Adam	318897	6165439	11/02–11/04	4.1	4.2	3.32
8	AW505500	Warren Reservoir	309409	6157186	10/03–11/04	4.8	5.3	3.99
9	Kyp02	Hallett Cove	273701	6115600	04/92–12/94	12.2	17.3	6.97
10	Kyp03	Bedford Park	278584	6121170	04/92–12/94	6.0	7.1	3.97
11	Kyp04	Happy Valley	279315	6115516	06/92–11/94	4.9	5.8	3.78
12	Kyp05	Flagstaff Hill	279991	6118507	06/92–12/94	6.5	7.0	5.10
13	Kyp06	Heathfield	292858	6120585	07/92–12/94	4.7	5.4	4.76
14	Kyp07	Hahndorf	300232	6121471	07/92–12/94	5.1	5.6	4.67
15	Kyp08	Mannum	345887	6135339	06/92–12/94	3.7	6.3	1.33
16	Kyp09	Murray Bridge	342703	6112274	06/92–12/94	6.1	8.3	2.54
17	Kyp10	Tailem Bend	359324	6097715	07/92–12/94	5.7	8.0	2.59

Note: simple mean is the arithmetic average of chloride concentration in the bulk precipitation samples regardless of the sample volume; while weight mean is the sample-volume weighted average of the bulk precipitation chloride concentration.

Title Page

Abstract

Introduction

Conclusions

References

Tables

Figures

◀

▶

◀

▶

Back

Close

Full Screen / Esc

Printer-friendly Version

Interactive Discussion



Chloride deposition mapping

H. Guan et al.

Table 2. Correlation matrix of chloride deposition and selected variables for sites #1–15 (P is annual precipitation, other symbols are described in Eq. 4).

	D	P	X	Y	Z	$\beta \cos(\alpha)$	$\beta \sin(\alpha)$
D	1						
P	0.48	1					
X	-0.81	-0.41	1				
Y	-0.61	-0.09	0.65	1			
Z	-0.03	0.79	0.19	0.44	1		
$\beta \cos(\alpha)$	0.09	0.05	-0.28	0.22	0.01	1	
$\beta \sin(\alpha)$	-0.41	-0.12	0.74	0.29	0.32	-0.67	1

Title Page

Abstract

Introduction

Conclusions

References

Tables

Figures

◀

▶

◀

▶

Back

Close

Full Screen / Esc

Printer-friendly Version

Interactive Discussion



Chloride deposition mapping

H. Guan et al.

Table 3. Regression results of chloride deposition with X , X and $\beta \sin \alpha$, respectively, based on observations of sites 1–15 (average mean annual chloride deposition of 3.94 g/m^2).

Predictor variables		b_0	$b_1 X$	$b_5 \beta \sin \alpha$	R^2	Adjusted ^a R^2	MAE ^b
X	coefficients	9.40	−0.054		0.65	0.62	0.63
	p values	1E-06	3E-04				
$X, \beta \sin \alpha$	coefficients	11.95	−0.075	7.72	0.73	0.68	0.54
	p values	0.0000	0.0003	0.090			

^a Adjusted coefficient of multiple determination considering the number of predictor variables effect.

^b MAE is the regression mean absolute error.

Title Page

Abstract Introduction

Conclusions References

Tables Figures

◀ ▶

◀ ▶

Back Close

Full Screen / Esc

Printer-friendly Version

Interactive Discussion



Chloride deposition mapping

H. Guan et al.

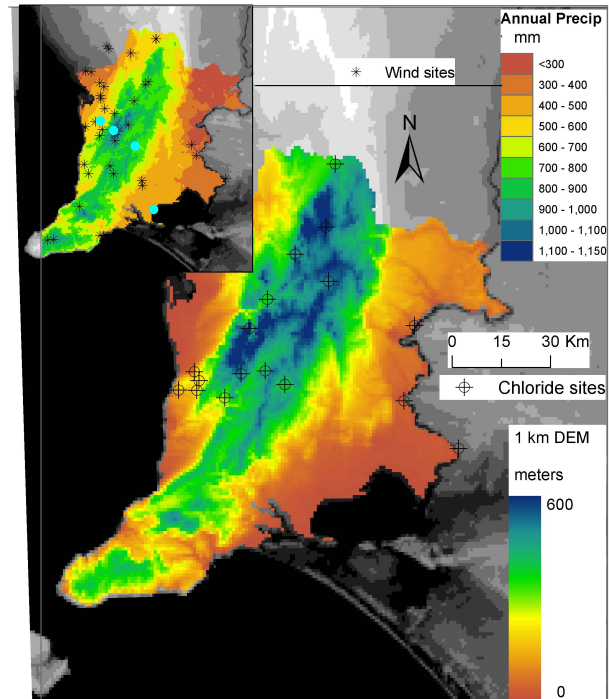


Fig. 1. The DEM map of the study area with 17 sampling sites (crossed circles) of bulk precipitation chloride, with an insert map of annual precipitation overlain by 41 wind observation sites (stars). The Bureau of Meteorology IDs of the four selected wind sites from northwest to southeast are 23 090, 23 733, 23 842, and 24 545.

Title Page

Abstract

Introduction

Conclusions

References

Tables

Figures

◀

▶

◀

▶

Back

Close

Full Screen / Esc

Printer-friendly Version

Interactive Discussion



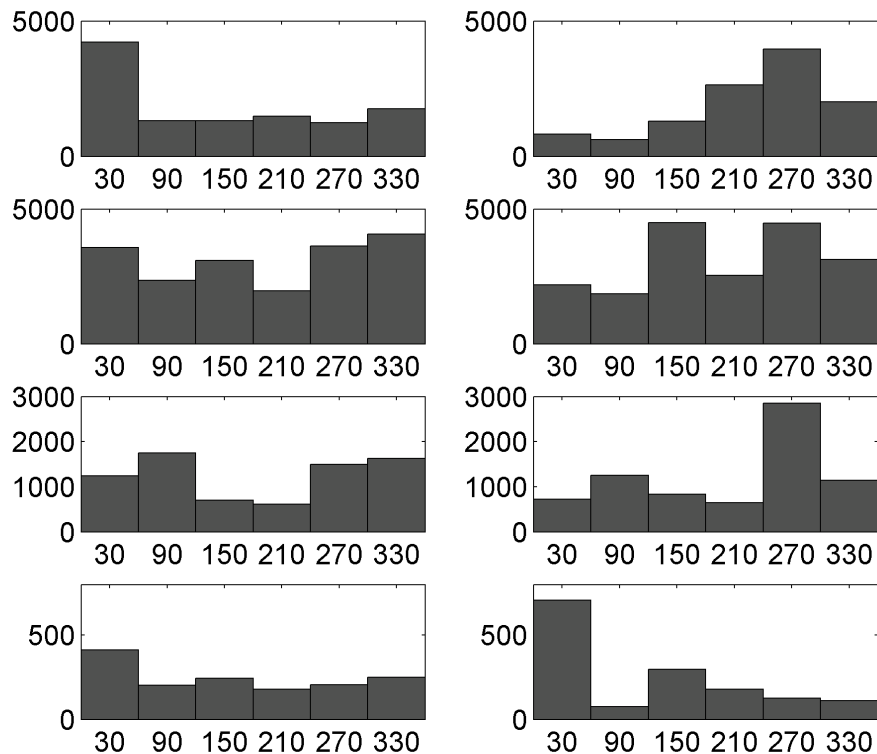


Fig. 2. Histograms of wind direction observed at 09:00 a.m. (left column) and 03:00 p.m. (right column) for four selected wind observation sites (23 090, 23 733, 23 842, and 24 545) (Fig. 1). Horizontal axis shows bin centres of the wind direction in degree clockwise from the north. The data were collected by BOM in 1977–2008, 1957–2008, 1987–2008, and 1965–1969 for the four sites, respectively.

Title Page

Abstract

Introduction

Conclusions

References

Tables

Figures

◀

▶

◀

▶

Back

Close

Full Screen / Esc

Printer-friendly Version

Interactive Discussion



Chloride deposition mapping

H. Guan et al.

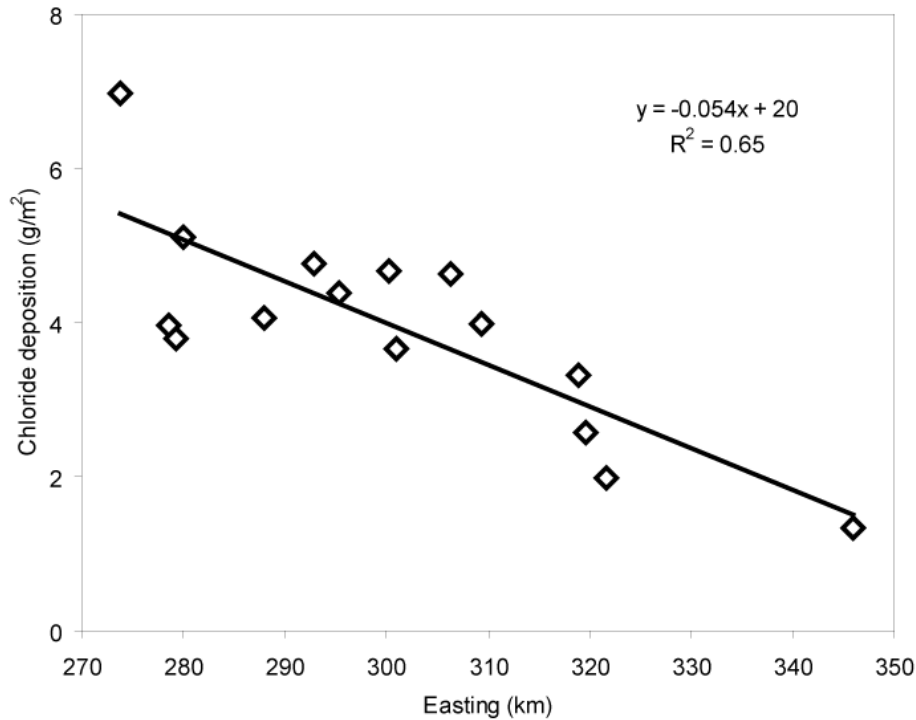


Fig. 3. Annual chloride deposition vs. UTM Easting (as a proxy for coastal distance), with sites #16 and #17 excluded.

Title Page

Abstract

Introduction

Conclusions

References

Tables

Figures

◀

▶

◀

▶

Back

Close

Full Screen / Esc

Printer-friendly Version

Interactive Discussion



Chloride deposition mapping

H. Guan et al.

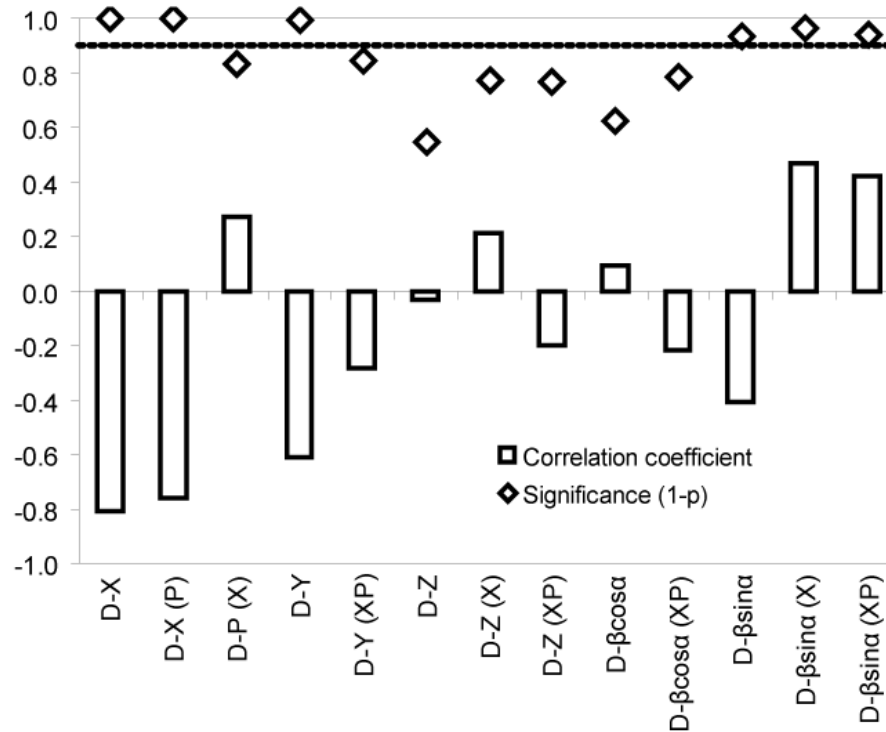


Fig. 4. (Partial) correlation coefficient between yearly chloride deposition and each of the selected variables, with or without the effects of other variables (specified in the bracket) removed, and the statistical significance ($1 - p$ value) of the linear correlation. The dash line is 90% significance for easy comparison between correlations.

Title Page

Abstract Introduction

Conclusions References

Tables Figures

◀ ▶

◀ ▶

Back Close

Full Screen / Esc

Printer-friendly Version

Interactive Discussion



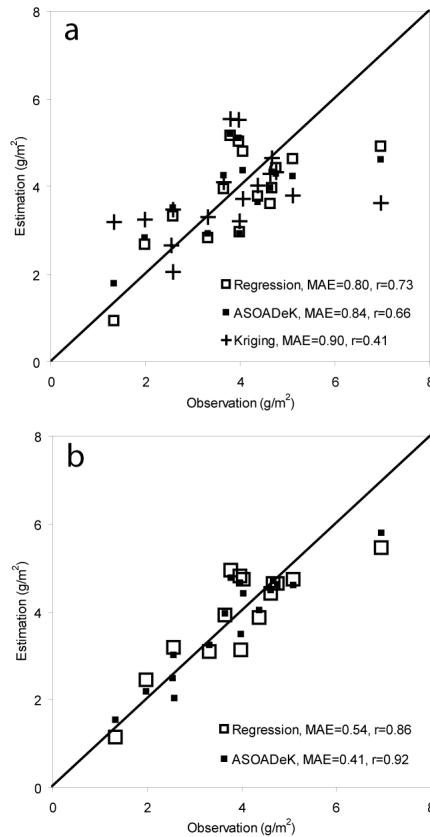


Fig. 5. (a) Cross-validation estimates of regression, ASOADeK, and direct ordinary kriging, and (b) regression estimates of annual chloride deposition (for the 15 sites) and ASOADeK estimates (for all 17 sites), in comparison to the observations. The MAE and r values are mean absolute error (g/m^2), and Pearson correlation coefficient between the estimates and the observations.

Title Page

Abstract

Introduction

Conclusions

References

Tables

Figures

◀

▶

◀

▶

Back

Close

Full Screen / Esc

Printer-friendly Version

Interactive Discussion



Chloride deposition mapping

H. Guan et al.

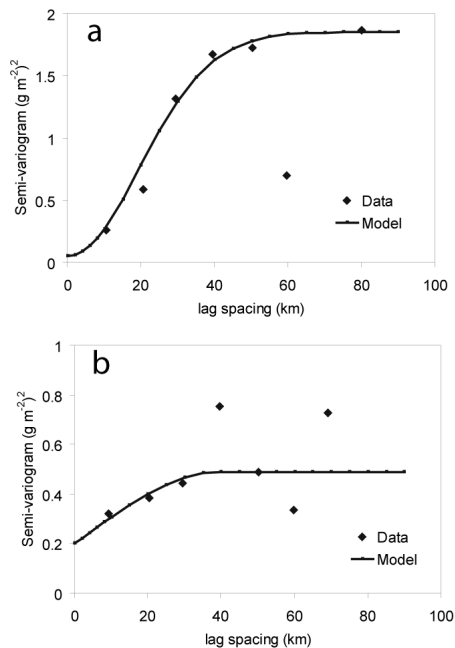


Fig. 6. Calculated semivariograms with a 10-km lag separation distance, and a 2-km lag tolerance, and model fitting for **(a)** observed annual mean chloride depositions, and **(b)** regression de-trended residuals over the 17 sites. The fitted model is a Gaussian model (range=48 km, sill=1.8 (g m⁻²)², and nugget=0.05 (g m⁻²)²) for (a), and a spherical model (range=40 km, sill=0.29 (g m⁻²)², and nugget=0.2 (g m⁻²)²) for (b).

Title Page

Abstract

Introduction

Conclusions

References

Tables

Figures

◀

▶

◀

▶

Back

Close

Full Screen / Esc

Printer-friendly Version

Interactive Discussion



Chloride deposition mapping

H. Guan et al.

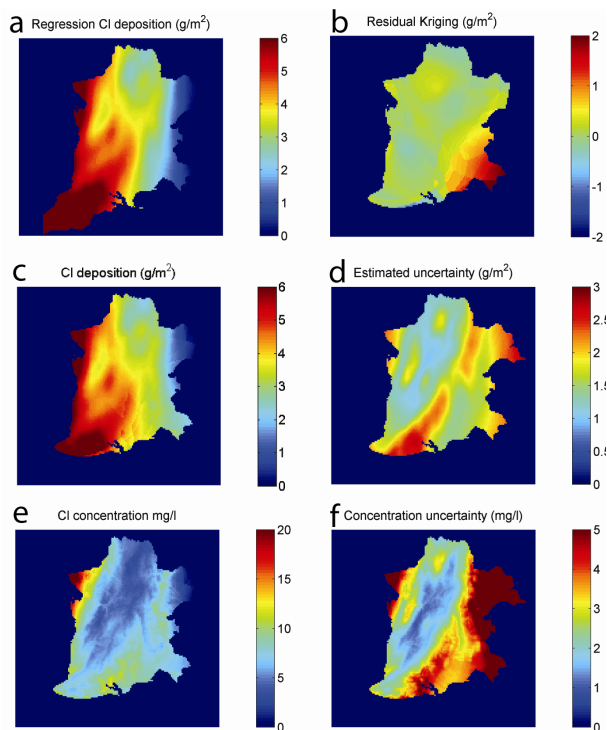


Fig. 7. Various mapping results of annual chloride deposition and related quantities over the study area: **(a)** regression map, **(b)** residual kriging map, **(c)** ASOADeK map, **(d)** ASOADeK map uncertainty, **(e)** bulk precipitation chloride concentration map, and **(f)** concentration map uncertainty.

Title Page

Abstract

Introduction

Conclusions

References

Tables

Figures

◀

▶

◀

▶

Back

Close

Full Screen / Esc

Printer-friendly Version

Interactive Discussion



Chloride deposition mapping

H. Guan et al.

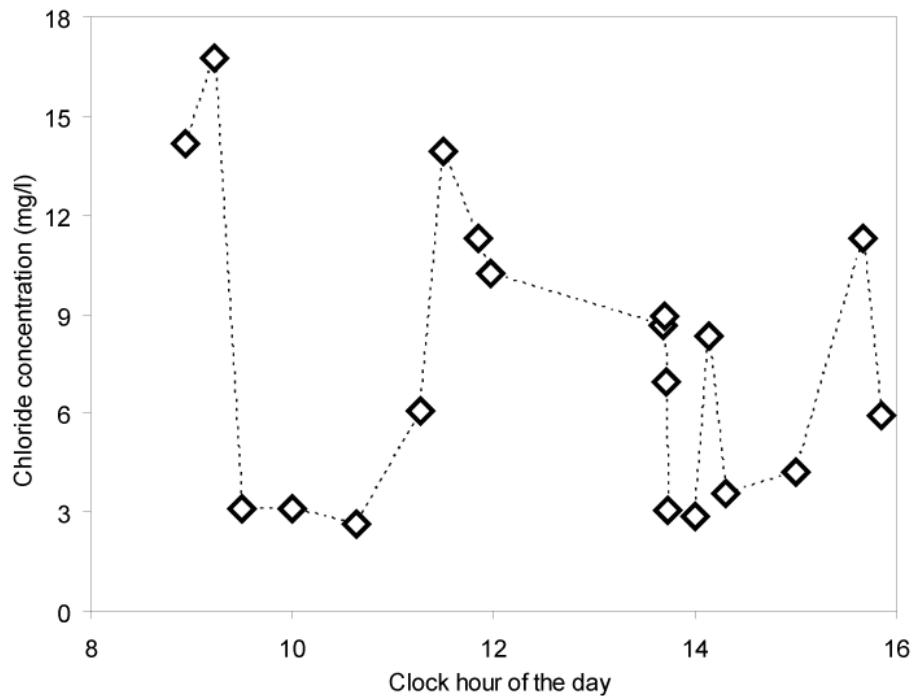


Fig. 8. Chloride concentration in each of the sequential 1.6 mm rain samples collected at Flinders University campus on 16 May 2008.

Title Page

Abstract Introduction

Conclusions References

Tables Figures

⏪ ⏩

◀ ▶

Back Close

Full Screen / Esc

Printer-friendly Version

Interactive Discussion



Chloride deposition mapping

H. Guan et al.

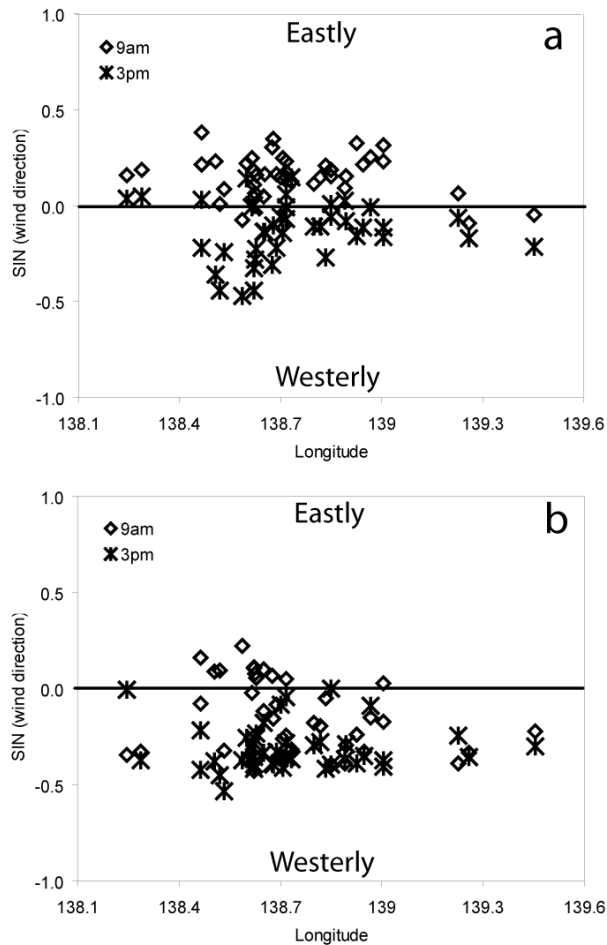


Fig. 9. Mean values of sin (wind direction) at the 41 observation sites (Fig. 1) for two seasons: **(a)** summer months (12, 1, 2), and **(b)** winter months (6, 7, 8).

Title Page

Abstract

Introduction

Conclusions

References

Tables

Figures

◀

▶

◀

▶

Back

Close

Full Screen / Esc

Printer-friendly Version

Interactive Discussion

